Influence of a $TiCl_4$ Post-Treatment on Nanocrystalline TiO_2 Films in Dye-Sensitized Solar Cells

P. M. Sommeling,*,† B. C. O'Regan,†,‡ R. R. Haswell,§ H. J. P. Smit,† N. J. Bakker,† J. J. T. Smits,§ J. M. Kroon,† and J. A. M. van Roosmalen†

Energy Research Centre of The Netherlands (ECN), Unit Solar Energy, Westerduinweg 3, 1755 LE Petten, The Netherlands, and Shell Global Solutions, Badhuisweg 3, CM 1031 Amsterdam, The Netherlands

Received: March 3, 2006; In Final Form: May 5, 2006

In this study, the influence of the $TiCl_4$ post-treatment on nanocrystalline TiO_2 films as electrodes in dye-sensitized solar cells is investigated and compared to nontreated films. As a result of this post-treatment cell efficiencies are improved, due to higher photocurrents. On a microscopic scale TiO_2 particle growth on the order of 1 nm is observed. Despite a corresponding decrease of BET surface area, more dye is adsorbed onto the oxide surface. Although it seems trivial to match this finding with the improved photocurrent, this performance improvement cannot be attributed to higher dye adsorption only. This follows from comparison between incident photon to current conversion efficiency (IPCE) and light absorption characteristics. Since the charge transport properties of the TiO_2 films are already more than sufficient without treatment, the increase in short circuit current density J_{SC} cannot be related to improvements in charge transport either. Transient photocurrent measurements indicate a shift in the conduction band edge of the TiO_2 upon $TiCl_4$ treatment. It is concluded that the main contribution to enhanced current originates from this shift in conduction band edge, resulting in improved charge injection into the TiO_2.

1. Introduction

Dye-sensitized solar cells based on nanocrystalline TiO_2 (DSC's) have attracted a lot of scientific and technological interest since their breakthrough in 1991.[1−3] The setup and working principle of this type of solar cell is very different from solar cells based on p−n junctions in semiconductor materials (e.g. silicon, CIS). The functionalities of charge generation and transport are no longer combined in one material but separated in different materials, i.e., a sensitizing dye, a (wide band gap) semiconductor (TiO_2), and a liquid redox electrolyte. One of the advantages of this build-up is that charge recombination in the bulk is effectively suppressed in comparison to the situation in the classical p−n junction. As a result, the semiconductor material is allowed to have a much lower purity than is usual for semiconductor materials. Knowing this, in combination with a foreseen simple processing of devices, low production costs are expected.[4,5] Although a low purity of TiO_2 can be tolerated, there are still opportunities for improvement of the properties of this material that is presently used in the DSC's.

A known method to improve the performance of the solar cells is a post-treatment of the TiO_2 film in which an extra layer of TiO_2 is grown onto the TiO_2 nanoparticles constituting the film. Different explanations of the working principle of this coating have been reported.[6−9] These hypotheses concern increased surface area,[6] improved electron transport,[6] light scattering,[7] TiO_2 purity,[8] and dye anchoring.[9] The post-treatment has been carried out using several TiO_2 precursors and methods: $TiCl_3$ electrodeposition[10] and titanium isopropoxide[11] and titanium tetrachloride ($TiCl_4$) post-treatment.[6−9,12] The latter results in the highest efficiency increase for the solar cells.[13]

In this study the post-treatment of nanocrystalline TiO_2 films with $TiCl_4$ and its effects on the TiO_2 properties and solar cell performance have been investigated. The effect on the cell performance is revealed by an increase in incident photon to current conversion efficiency (IPCE) and short circuit current density (J_{SC}) of typically 10−30% relative to untreated films. The IPCE of a solar cell is influenced by three factors: light harvesting efficiency (LHE) of the colored TiO_2 film, electron injection efficiency (Φ_{INJ}) of the excited dye into the TiO_2, and the collection efficiency of the injected electrons to the TCO (Φ_{COLL}). The relation between these factors is given by

$$\mathrm{IPCE} = \mathrm{LHE} \times \Phi_{INJ} \times \Phi_{COLL}$$

Two of these three factors can be split up as follows in more detail:

LHE is resulting from TiO_2 surface area, dye loading, and light scattering/reflection events. Surface area is the total internal surface area of the TiO_2 film, and the dye loading is dependent on the number of specific binding sites on TiO_2 for the sensitizer. Light scattering influences the optical absorption of a film and can contribute to a higher performance.

Φ_{COLL}, the charge collection efficiency, is related to the ratio of charge transport through TiO_2 and charge recombination: $\Phi_{COLL} = K_t/(K_t + K_r)$, with K_t and K_r being the rate constants for transport and recombination, respectively.

In this study the observed increase in IPCE after $TiCl_4$ treatment has been investigated by analysis of these five factors: surface area, dye loading, light scattering, charge

* Corresponding author. Tel: +31 224 564276. E-mail: sommeling@ecn.nl.

† Energy Research Centre of The Netherlands (ECN).

‡ Present address: Centre of Electronic Materials and Devices, Department of Chemistry, Imperial College, London, Exhibition Road SW7 2AZ, U.K.

§ Shell Global Solutions.

10.1021/jp061346k CCC: $33.50
Published on Web 09/08/2006

transport, and charge recombination. The first three factors will be considered in the sections about materials characterization and optical analysis of TiO_2 films (sections 3.1 and 3.2). Charge transport and recombination will be treated in the section about photoelectrical characterization of DSC (section 3.3).

2. Experimental Methods

2.1. Synthesis of Titanium Dioxide Colloids (TiO_2) and Preparation of Screen Printable Paste. TiO_2 colloids have been synthesized from titanium isopropoxide precursor according to procedures published earlier.[14] In short, 58.6 g of titanium isopropoxide is mixed with 12 g of concentrated acetic acid and stirred for 15 min. The mixture is poured into 290 mL of water and stirred for 1 h. Then 4 mL of HNO_3 (65%) is added under stirring. The mixture is heated to 80 °C and stirred for 1.5 h at 80 °C under reflux. After cooling, the colloidal solution that has formed is transferred to a titanium autoclave and heated at 230 °C for 12 h. The TiO_2 colloid is transferred from the aqueous solution into a terpineol/ethylcellulose mixture to obtain a screen printable paste using a pearl mill. TiO_2 films have been screen printed onto TCO-coated glass.

2.2. Fabrication of Solar Cells, Processing of Master Plates. Master plates have been applied as a research vehicle. A master plate consists of two SnO_2:F-coated glass plates (7.5 $\times$ 10 cm^2, LOF tec 8) on which five electrically isolated electrodes (area 4 cm^2) are deposited by screen printing. One glass plate contains five TiO_2 photoelectrodes. To enhance the light absorption, an additional TiO_2 film consisting of 300 nm scattering particles (Fluka) has been applied to a part of the cells.[6,15] The other glass plate contains five platinum (Pt) counter electrodes. The active layers (TiO_2 and Pt) are dried and fired at 570 and 450 °C for TiO_2 and Pt, respectively, to remove all organic components and to establish sufficient interparticle contacts between the TiO_2 particles. A typical film thickness of 10−12 μm TiO_2 is obtained after firing. The thickness of the light scattering film is typically 5 μm. The two glass plates comprising the photoelectrode and counter electrodes are laminated together using hotmelt foils such as Surlyn or Bynel. Further details are reported elsewhere.[4,15−16]

For all experiments *cis*-bis(isothiocyanato)bis(2,2′-bipyridyl-4,4′-dicarboxylato)ruthenium(II) bis(tetrabutylammonium) (N719, Solaronix S. A.) has been used as a sensitizer for TiO_2 electrodes. Solvents and additives hexylmethylimidazolium iodide (HMI, DSM), *tert*-butylpyridine (TBP, Aldrich), lithium iodide (LiI, Aldrich), guanidinium thiocyanate (Aldrich), and iodine (I_2, Aldrich) have been used as received without further purification.

The electrolyte used for performance and IPCE measurements consisted of 0.6 M HMI, 0.1 M LiI, 0.05 M I_2, and 0.5 M TBP in acetonitrile (ACN). For the cells tested in the transient measurements (section 2.7), the electrolyte compositions were as follows: electrolyte Gu, 0.6 M PMII, 0.1 M guanidinium thiocyanate, 0.05 M I_2, 0.5 M TBP in ACN; electrolyte Li, 0.6 M PMII, 0.1 M LiI, 0.05 M I_2, 0.5 M TBP in ACN; electrolyte HLi, 0.5 M LiI, 0.05 M I_2, 0.5 M TBP in ACN.

2.3. $TiCl_4$ Post-Treatment. The post-treatment with $TiCl_4$ has been applied to freshly sintered TiO_2 films according to literature procedures.[12] An aqueous stock solution of 2 M $TiCl_4$ was diluted to 0.05 M. Sintered electrodes were immersed into this solution and stored in an oven at 70 °C for 30 min in a closed vessel. After flushing with demineralized water and drying, the electrodes were sintered again at 450 °C for 30 min. For the determination of the increase in mass of the TiO_2 electrodes, a control group has been subjected to a similar process, only leaving out the $TiCl_4$ in the dipping bath. The profiles and film thickness for TiO_2 films have been determined using a Dektak 8 stylus profilometer (Veeco Instruments).

2.4. Materials Characterization by XRD, TEM, and BET. XRD measurements have been conducted using Bruker D8 Advance equipment following the Bragg Brentano measurement method. TEM analyses were made using a JEOL 2010 transmission electron microscope operated at 200 keV with a LaB_6 filament. The TEM analysis of treated and untreated particles has been made by scraping off TiO_2 films and subsequently suspending them in a solvent. BET determination (single point BET) has been carried out using a Carla Erba Strumentazione, Sorpty 1750.

2.5. Optical Studies. Dye desorbtion experiments have been carried out using screenprinted TiO_2 films with and without $TiCl_4$ post-treatment. These films have been coated with N719 dye from a 0.3 mM ethanolic solution. For each sample the dye was desorbed from the electrodes by treating with a quantified amount of diluted (0.13 M) NH_3 in water, resulting in a dye solution of which a UV/vis (Hewlett-Packard 8453 UV/vis spectrophotometer) spectrum has been recorded. A correction for small variations (introduced by the screen printing process) in film thickness has been made by dividing the absorbance of each dye solution by the film thickness of each corresponding TiO_2 electrode. Since the absorbance is linearly related to the concentration of dye and for all samples the dye has been desorbed into equal volumes of diluted NH_3, the relative difference in absorbance directly translates into the relative difference in dye loading of the TiO_2 surface. Light absorption characteristics have been determined by reflection/transmission measurement using an integrating sphere.

2.6. IV and IPCE Characterization. IV measurements have been carried out using a Steuernagel constant 575 solar simulator (equipped with 575 W metal halide lamp) and a Keithley 2400 source meter. Calibration of this system has been carried out by comparative measurements of DSC's with a Spectrolab X-10 solar simulator. IPCE measurements have been carried out according to the ASTM E1021-84 norm.[17−18] A 1000 W xenon lamp (Osram XBO/HS OFR) was used as a light source in combination with small band-pass filters (Schott, fwhm = 6−10 nm) to generate monochromatic light. The monochromatic light was passed through a chopper wheel to create a small modulated signal on top of a constant signal originating from 0.5 to 1 sun bias illumination. The resulting modulated current is analyzed by a lock-in amplifier.

2.7. Transient Photovoltage and Photocurrent Measurements. The effect of the $TiCl_4$ treatment on electron transport has been examined by measuring photocurrent transients under short circuit conditions. In these measurements, the bias light was modified to give approximately the same photocurrent for each cell, since the photocurrent transient is dependent on the magnitude of the photocurrent. Photocurrent and photovoltage transients were taken using a pump pulse generated by an array of red LEDs controlled by a fast solid-state switch. Pulse times of 100 μs were used, with a rise and fall time of <1 μs. The pulse was incident on the SnO_2 side of the cell. The pulse intensity was controlled to keep the ΔV due to the pulse below 10 mV. White bias light, incident on the SnO_2 side of the cell, was supplied by 10 W Solarc lamps (WelchAllyn). The bias light was attenuated when needed by neutral-density filters. The time resolution of the potentiostat was 20 μs; all transient were 200 μs or longer.

The transient voltage data have been used to calculate the capacitance at each V_{OC}. The procedure has been described

TABLE 1

Change of TiO_2 Characteristics after $TiCl_4$ Treatment

					particle diameter (nm)	
	BET (m^2/g)	TiO_2 mass[a] (mg/cm^2)	electrode surf. area[b] (m^2)	porosity[c] (%)	from TiO_2 mass[d]	from TEM[e]
TiO_2	72	1.56	0.449	70	na	13.1
TiO_2 after $TiCl_4$	53	2.00	0.424	63	na	15.7
change (%)	−26.4	+28	−6	−10	+8.6	+20

Change in IV Parameters after $TiCl_4$ Treatment[f]

	J_{SC} (mA/cm^2)	V_{OC} (V)	FF	η (%)
TiO_2	9.5 ± 0.2	0.68 ± 0.01	0.67 ± 0.004	4.3 ± 0.1
TiO_2 after $TiCl_4$	11.2 ± 0.2	0.69 ± 0.01	0.66 ± 0.004	5.1 ± 0.1
change (%)	+18	+1.5	−1.5	+19

[a] TiO_2 mass has been determined on 4 cm^2 electrodes and is expressed in mg/cm^2 geometrical electrode area. [b] Electrode (internal) surface area has been calculated by multiplication of BET and TiO_2 mass, for a 4 cm^2 film. [c] Porosity has been determined by calculating the overall density of a 4 cm^2 TiO_2 film from the TiO_2 mass, taking 13 μm film thickness and comparison to a density of 4.2 g/cm^3 for bulk TiO_2. [d] Calculated from TiO_2 mass increase assuming spherical particles. [e] Particle diameters from TEM are based on measurement of diameters on TEM photographs (175 particles for each measurement). Statistic analysis reveals that the difference in particle diameter is significant at the 95% confidence level. [f] The IV measurements have been conducted on 4 cm^2 cells (without scattering layer) at a lamp intensity corresponding to 0.94 sun.

elsewhere.[19] Briefly, the capacitance of the TiO_2/electrolyte interface can be calculated as $C = \Delta Q/\Delta V$, where ΔV is the peak of the transient and ΔQ is the number of electrons injected by the pulse. We find ΔQ by integrating a photocurrent transient at $V = 0$, caused by an identical pulse.

The following procedure was used to measure the recombination rate at short circuit.[20] The cell is placed under a given illumination. The attached potentiostat (galvanostatic mode) is set to supply a constant current equal to the short circuit current that the cell is generating. A light pulse is applied and the voltage transient that results is measured. When the constant current is set, a potential near $V = 0$ is maintained at the SnO_2 contact. When a light pulse is applied, the galvanostat must increase the voltage to counter the increase in current that would be caused by the increase in the photoinjected electron concentration in the porous TiO_2 film. Because the current and bias light are constant, the excess electrons can only leave the TiO_2 by recombination. The decay of the transient voltage thus measures the recombination rate relevant to short circuit current flow.

3. Results

3.1. Materials Characterization of the TiO_2 Films. The effects of the $TiCl_4$ treatment on TiO_2 films have been studied by BET, weight analysis, profilometry, XRD, and TEM. The results of these measurements are summarized in Table 1, also including the results of the IV measurements, as described in section 3.3.

Some obvious effects of the $TiCl_4$ treatment are a decrease in BET surface area and an increase in particle diameter and mass of the treated TiO_2 films. The average decrease in mass for the control group, which has gone through an equal process, only leaving out the $TiCl_4$ in the dipping bath, is 2.7%. This indicates that the measured increase in mass after the $TiCl_4$ treatment is significant and accurate. The small loss in mass of this control group can be attributed to a slight flaking of the TiO_2 film. To verify if the increase in TiO_2 mass is related to an increased TiO_2 film thickness, surface profiles of treated and nontreated films have been measured (Figure 1).

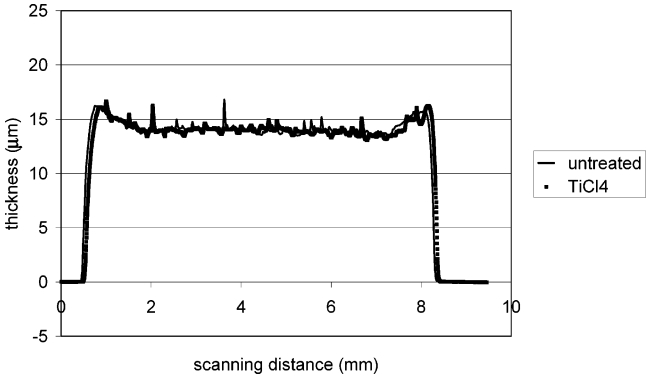

Figure 1. Profiles of TiO_2 films before and after treatment with $TiCl_4$.

Comparison of the profiles indicates that, apart from occasional local TiO_2 clusters, no increase in TiO_2 film thickness results from the treatment, as is shown in Figure 1.

From these observations it follows that, despite the substantial decrease in BET surface area, the loss in actual electrode surface area after $TiCl_4$ treatment is only 6% (from 0.449 to 0.424 m^2) because of the increase in mass of TiO_2 on the electrode. Since the film thickness is not affected, the porosity must have decreased, as is shown in Table 1.

From the increase in mass an increase in particle diameter of 8.6% has been calculated by assuming spherical particles, as shown in Table 1. From TEM measurements an increase in average particle diameter of 20% has been calculated.

No obvious difference can be seen between treated and untreated TiO_2 from the TEM photographs (Figure 2); however, by determination of a large number of particle diameters from the TEM photographs, a significant difference is observed, as follows from Figure 3 and is included in Table 1.

By X-ray diffraction an estimation of the primary particle size of the TiO_2 particles has been made. After $TiCl_4$ treatment the particle size is increased; the increase, however, could not be quantified. From XRD no obvious change in the rutile content (20−25%) of the TiO_2 could be observed, nor any other morphological changes; i.e., the formation of an amorphous phase or the presence of small crystallites was not observed.

3.2. Optical Analysis of TiO_2 Films. For $TiCl_4$ treated and untreated TiO_2 films dye has been adsorbed and desorbed from the electrodes by treating with diluted NH_3, resulting in a dye solution of which a UV/vis spectrum has been recorded; see Figure 4.

The difference between $TiCl_4$-treated and nontreated TiO_2 is distinctive, showing a 7.6% higher dye loading for $TiCl_4$-treated electrodes.

To verify what is effectively changed in the TiO_2 film optical behavior by a higher dye load, optical analyses of colored TiO_2 films have been conducted using an integrating sphere (Figure 5).

The light absorption and reflection characteristics of colored TiO_2 films reveal that there is hardly any visible effect of the $TiCl_4$ treatment in the absorption maximum (550 nm) of the dye. This is because the light absorption is already saturated around this maximum, even without $TiCl_4$ treatment.

3.3. Photoelectrical Characterization of DSC. *IV Characterization and IPCE Measurements.* The beneficial effect of the $TiCl_4$ post-treatment on different IV parameters is presented in Table 1. The increase in current density and overall cell efficiency upon $TiCl_4$ treatment is 18% and 19%, respectively.

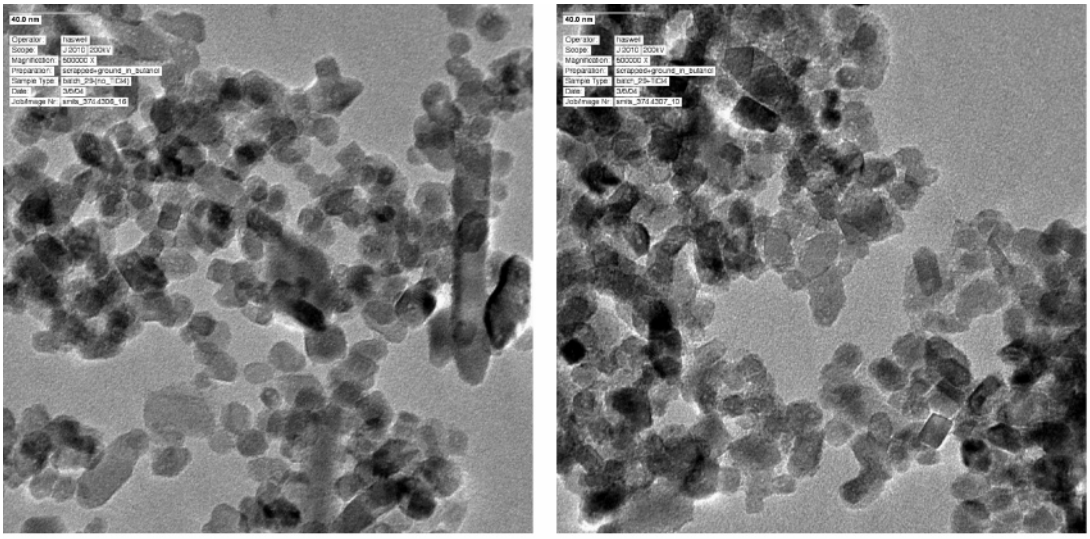

TiO_2 particles, magnification 500.000 times

TiO_2 particles after $TiCl_4$ treatment, magnification 500.000 times

Figure 2. TEM photographs of TiO_2 particles with and without post-treatment with $TiCl_4$.

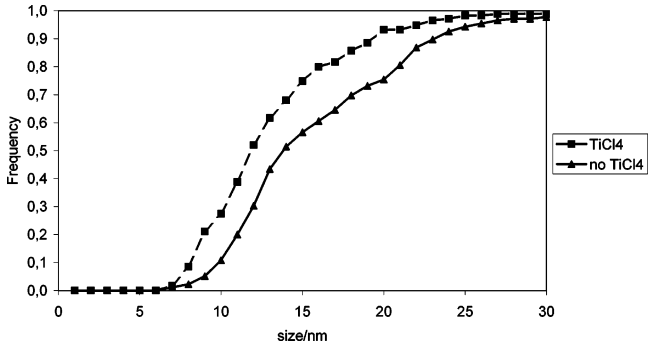

Figure 3. Histogram of the particle distribution derived from the TEM photographs presented in Figure 2.

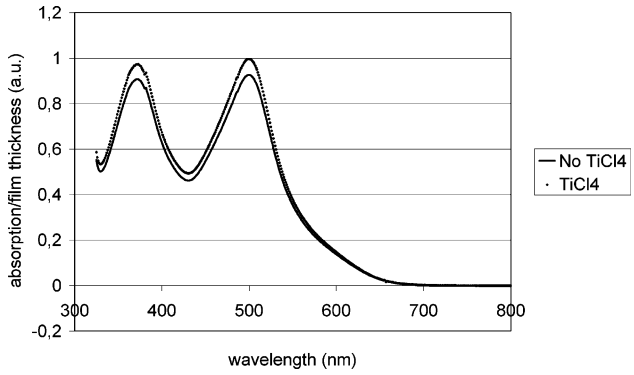

Figure 4. Absorbance of aqueous dye solutions after desorption from TiO_2 films. The curves are normalized taking into account small differences in film thicknesses of the samples, originating from screen printing, by dividing the absorbance by the film thickness. Both curves represent the average of three samples. The difference in absorbance at 500 nm is 7.6% (±0.07).

The increase in solar cell performance completely originates from the increase in current density; V_{OC} and FF are not affected.

To analyze in more detail the enhanced short circuit current, IPCE measurements have been conducted. The results are presented in Figure 6.

IPCE curves for $TiCl_4$-treated cells reveal an upward shift with respect to nontreated cells in the wavelength range from

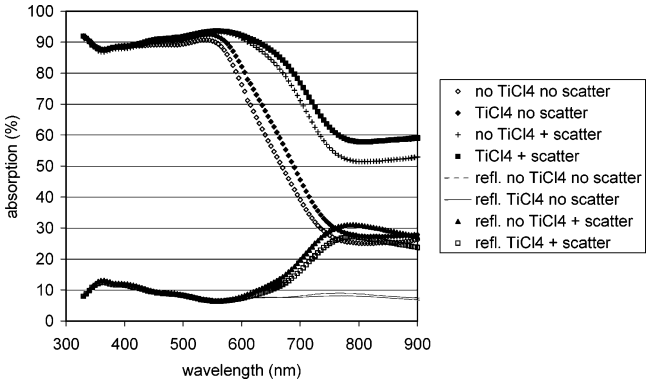

Figure 5. Light absorption of stained TiO_2 films (N719) with and without scattering layer and $TiCl_4$ treatment. The absorption has been derived from reflection transmission measurements using an integrating sphere. Reflection data have been added in the graph. Note: the nonzero absorption in the region from 800 nm onward is mostly due to the absorption of the TCO (in combination with the scattering properties of the films), as has been verified with noncolored films. The absorption maximum is approximately 93% because of a minimum reflection of 6−7% of the samples.

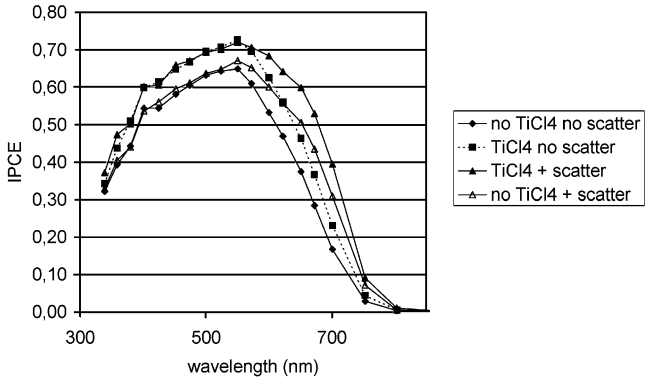

Figure 6. IPCE curves of cells before and after $TiCl_4$ treatment with and without scattering layer.

350 to 800 nm, both for scattering and nonscattering films. The additional scattering layer induces an upward shift in the wavelength region between 550 and 800 nm, both for $TiCl_4$ treated and nontreated films. From the IPCE curves, J_{SC} has

TABLE 2: Electron Transport Time Compared with Steady State Photocurrent Increase for DSC with and without $TiCl_4$ Treatment

	photocurrent transient half time (μs)[a]		I_{PHOTO} increase
electrolyte	no $TiCl_4$	$TiCl_4$	(%)
Gu	740	740	33
Li	880	680	28
HLi	950	910	26

[a] Measured with white bias light intensity 70−90 mW/cm^2 varied to give identical steady-state current. Values are the average of two or three separate cells. Electrolyte compositions are described in the Experimental Section. Thin (3 μm) TiO_2 layers were used in these cells to avoid RC limitation of the photocurrent transients; these thinner layers showed larger improvements from the $TiCl_4$ treatment than the thicker layers used for IV and IPCE measurements.

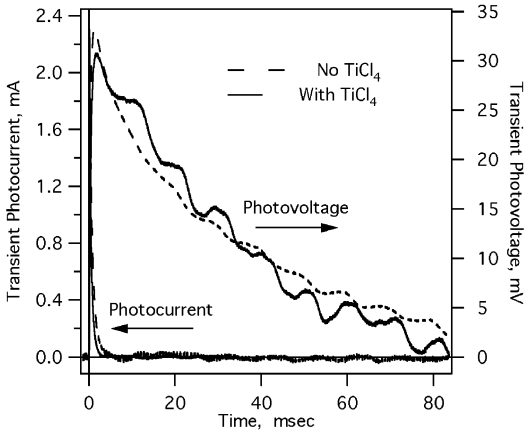

Figure 7. Transient photocurrent and transient photovoltage at short circuit for two matched cells with and without $TiCl_4$ treatment.

been calculated for these cells by convolution of the IPCE with the AM 1.5 G solar spectrum and subsequent integration. The deviation between these calculated values and measured J_{SC} under standard testing conditions (class A solar simulator, AM 1.5 G, 1000 W/m^2) is small (0.7−3.2%). This shows that the IV and IPCE data are in good agreement.

Transient Photovoltage and Photocurrent Measurements. Transient measurements have been applied to examine charge transport and recombination. Table 2 shows the photocurrent transient lifetimes (1/e) for cells with and without $TiCl_4$ treatment and three different electrolytes. The change in 1 sun photocurrent for these particular pairs of cells is included.

As can be seen from Table 2, $TiCl_4$ treatment changes very little in the charge transport for two of the cases, and in the third case there was a 22% decrease in the transport time.

To further investigate the electron transport, we have compared the transport lifetime and the recombination lifetime under short circuit conditions. Figure 7 shows representative transport and recombination transients for a matched pair of cells, with and without $TiCl_4$.

The capacitance versus voltage of the cells with and without electrolyte was also measured. Figure 8 gives these results for two matched (with and without $TiCl_4$) pairs of cells. In each case a strong shift in the capacitance curve is apparent for the $TiCl_4$-treated cells. The capacitance of the TiO_2/electrolyte film is proportional to the differential density of states (DOS) at the Fermi level in the TiO_2 particles.[19,21−22] The right axis on Figure 8 shows the DOS calculated for these films using DOS = 6.24 × 1018 × $C/(d(1 - p))$, where C is the capacitance/cm^2, d is

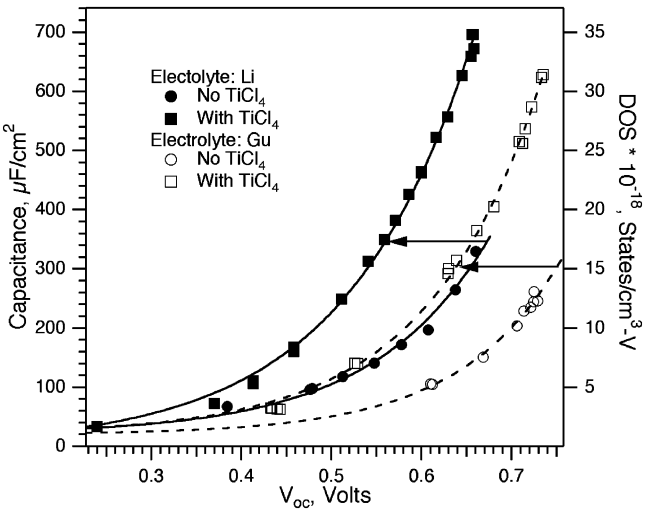

Figure 8. Capacitance versus voltage of DSC with and without $TiCl_4$ treatment for two matched pairs of cells with different electrolytes.

the thickness of the TiO_2 film in cm, p is the porosity, and the conversion factor is the number of electrons per coulomb.

4. Discussion

As mentioned in the Introduction the IPCE of a DSC is a result of light harvesting efficiency (LHE), charge injection efficiency (Φ_{INJ}), and collection efficiency (Φ_{COLL}). For a given dye and absorption coefficient, LHE can be split into three contributing factors: surface area, dye loading, and scattering effects. Φ_{COLL} can be interpreted in terms of rates for transport (K_t) and recombination (K_r) in the following way: $\Phi_{COLL} = K_t/(K_t + K_r)$. The results described in the previous section will be discussed here in relation to these five factors.

4.1. Effects of the $TiCl_4$ Treatment on TiO_2 Morphology and Surface Area. The increase in photocurrent for TiO_2 layers that are treated with $TiCl_4$ in comparison to nontreated layers has led to speculations on increased dye adsorption due to an increase of the TiO_2 surface area.[6] Also an increased layer thickness has been suggested as a reason for increased LHE.[7] In the present investigation, it is shown that the net effect of the $TiCl_4$ treatment is a significant mass increase of the TiO_2 films with 28%. The $TiCl_4$ procedure does not influence the layer thickness, from which it can be concluded that all changes take place inside the film.

The only observable change in the X-ray diffraction pattern is line broadening, indicating particle growth. There are no indications that the $TiCl_4$ treatment results in the growth of small crystallites or an amorphous phase. This is supported by the decrease of the BET surface area. The TEM measurements indicate no morphological changes either. From the TEM recordings, particle growth from 13.1 to 15.7 nm is observed. The overall conclusion from these observations is that the $TiCl_4$ treatment leads to a growth of the TiO_2 particle radius of about 1 nm. The indications are that the growth is epitaxial.

The result of the $TiCl_4$ treatment is growth of the TiO_2 particles and a consequent decrease in BET surface area of about 26%. If the decrease in BET surface area (measured in m^2/g) is combined with the increase in mass of 28%, this results in an overall decrease of the electrode surface area of approximately 6%. This means that the changes due to the $TiCl_4$ treatment on the TiO_2 morphology a priori do not provide any indications for the observed increase in photocurrent, since one would

expect a decrease of the electrode surface area to result in lower dye adsorption and decreased LHE.

4.2. Dye Adsorption and Photocurrent Generation. However, on the contrary, the effect of the $TiCl_4$ treatment does result in a distinctive increase in dye adsorption. The dye desorption experiments (Figure 4) show that the $TiCl_4$-treated electrodes adsorb 7.6% more dye than the nontreated electrodes, despite the 6% lower surface area. The morphological studies do not provide data to accommodate this. This suggests that the reasons for the higher dye absorption are to be found on a different scale than can be seen with X-ray and TEM. Presumably, the TiO_2 surface after the $TiCl_4$ treatment provides more specific binding sites.[13] Potentially, the $TiCl_4$ treatment also reduces the fraction of the TiO_2 surface area that is inaccessible for the dye due to sterical constraints.

The relation between more dye and more current seems obvious, and indeed, it has been reported to be the main reason for the observed increase in photocurrent due to the $TiCl_4$ post-treatment.[6,8,12] However, a further analysis shows that only a part of the increase in photocurrent can be ascribed to the increased amount of dye, as is discussed below.

In Table 1, the IV data show that the increase in current due to the $TiCl_4$ treatment is 18%, whereas for these films a higher dye loading of 7.6% was observed (Figure 4). It is obvious that the increase in current is much more than can be ascribed due to the increase in dye loading. Moreover, the light absorption of films of this thickness is almost completely saturated in the absorption maximum of the dye, as was confirmed by determination of light absorption of the films (Figure 5). More dye in this case would not result in more current in the absorption maximum. It could only result in an improved red response, similar to what would happen if the layer thickness would be increased or if a scatter layer would be applied (see below).

To quantify this, the IPCE spectra of the cells were recorded. From Figure 6 it can be seen clearly that the IPCE curve shifts upward over the entire wavelength range upon the $TiCl_4$ treatment, as was also reported earlier.[10,13] Further evidence comes from the IPCE measurements on similar layers but now equipped with an additional scatter layer on top. The effect of scattering clearly results in a much larger improvement of the red response than originates from the higher dye loading. Also for the films with scatter layer the entire IPCE curve is shifted upward. This upward shift in IPCE is 8% in the absorption maximum, which is in sharp contrast to a corresponding increase in light absorption of only 0.25%. It follows that other factors than the increased LHE play a role in the improved solar cell performance.

However, it should be noted that the enhanced photocurrents and IPCE values in the present study are lower than for the record cells,[12] so there is still opportunity for efficiency improvement.

In summary, although it is not expected on the basis of the observations discussed in section 4.1, the dye adsorption of TiO_2 is improved by $TiCl_4$ treatment. However, the photoelectrical analysis of the films shows that the contribution to an enhanced LHE is minor and the higher quantity of adsorbed dye is not the major contribution to the observed improvement in IPCE. This leaves Φ_{INJ} and Φ_{COLL} as candidates for IPCE improvement, as will be discussed in the next section.

4.3. Relation between Charge Transport, Recombination, and IPCE. As can be seen from the photocurrent transient lifetimes (Table 2), $TiCl_4$ treatment changes very little in the charge transport rate (K_t) for two cells. For the third cell, there was a 22% decrease in the transport time. Since the cells with no change in transport show the largest improvement in photocurrent, it is apparent that, in general, an increase in electron transport is not the mechanism by which photocurrent was increased.

To further support this, we have compared the transport lifetime and the recombination lifetime under short circuit conditions. Figure 7 shows representative transport and recombination transients for a matched pair of cells, with and without $TiCl_4$. It is clear from the transients that the transport under short circuit conditions is much faster than the recombination, and thus no losses to recombination are occurring at short circuit. More quantitatively, the recombination lifetime is about 40 ms, where the transport half times are about 900 and 700 μs. Under these conditions, about 2% of the charges are lost to recombination, so $\Phi_{COLL} = K_t/(K_t + K_r)$ is close to unity. Thus, even if large improvements in transport had been measured, they could not have been responsible for the increase in short circuit photocurrent observed. It can be concluded that Φ_{COLL} is not increased by the $TiCl_4$ treatment. This only leaves Φ_{INJ} as a candidate for improvement of IPCE/current. In the following sections this will be related to an observed shift in conduction band edge.

The density of states (DOS) versus voltage has been measured for cells with and without $TiCl_4$. Figure 8 shows these results for two matched pairs of cells. In each case there is a strong shift in the DOS curve. The leftward shift along the V_{OC} axis is most likely the result of a shift of the TiO_2 band edge downward toward the I_3^-/I^- potential. The downward shift of the conduction band causes a given DOS to appear at a lower V_{OC}, as V_{OC} is measured up from the iodine/iodide potential. From the data, the magnitude of the shift is approximately 100 mV. Such a shift would imply that the surface potential of the TiO_2 is more positive in the cells with $TiCl_4$ treatment. This will cause a change in the surface dipole, to point more in the direction of the TiO_2, moving the band edge down. The $TiCl_4$ treatment could cause this effect in several ways: For example, it may be that the crystal face exhibited by the $TiCl_4$-treated TiO_2 is different from that expressed on the autoclaved particles. This could give rise to a stronger binding of protons and/or other cations. In any case, a 100-mV shift in the conduction band could be significant enough to increase the rate and the quantum efficiency of electron injection from the excited dye.

Alternatively, the shift in the DOS curves in Figure 8 could be viewed as an increase in the trap density rather than a shift of the conduction band. Interpreted in this way, the $TiCl_4$ treatment increases the trap density by a factor of $\sim$2.3 across the whole voltage range. Several factors argue against this interpretation. Since the $TiCl_4$ treatment only increases the TiO_2 mass by a factor of 1.4, an overall increase in traps of a factor 2.3 would imply that the $TiCl_4$ deposited TiO_2 has a trap state density that is 3.5 times higher than the original TiO_2 particles, which is unlikely. Moreover, such a large increase in trap density would be expected to slow the transport, which is not observed, and to increase the amount of charge stored in the film under short circuit conditions, which is also not observed. A shift in band edge is the most probable explanation. Further discussion of this question will be given in a coming paper.[23]

It may be noted that a downward shift in the conduction band should give a lower V_{OC}. This does not occur because the $TiCl_4$ treatment also acts to strongly reduce the recombination rate. This has been mentioned in the literature, and we have confirmed a 30-fold reduction in the recombination rate for a given DOS in the cells used in this study.[23−24] The reduction in the recombination rate allows the 1 sun flux of injected

electrons to build up a higher density of charge in the TiO_2 (see Figure 8). This effect compensates for the downward movement of the band edge.

5. Conclusions

Our observations show an increase in photocurrent that is primarily not caused by an increase in light absorbed or by a decrease in losses during transport. From this we can conclude that, in the untreated films, some absorbed photons do not result in electron injection into the TiO_2 conduction band. Our data do not preclude that some electrons are injected into surface states, which then recombine geminately with the dye. One explanation for some excited dye molecules failing to inject would be a conduction band potential that was near or above the oxidation potential of the excited dye. In this case, the electron injection rate could be slow enough that other reactions can compete with injection to some extent. Under this explanation, a downward shift in the band edge would be expected to give a higher quantum efficiency of injection and thus a higher photocurrent, as observed.[25]

It is also interesting to note that the efficacy of the $TiCl_4$ treatment has been found to vary widely, depending on the source and history of the particles used to make the film. This would be expected if the source of the increased photocurrent is a shift in the band edge. If, for a given particular film, the band edge was already at the correct potential to maximize the quantum efficiency of injection, then further shifts caused by the $TiCl_4$ treatment would not be beneficial. In other words, when the photocurrent is already high without the treatment (corresponding to cell efficiencies around 10%), the improvements with $TiCl_4$ are limited.[12]

Acknowledgment. The authors thank Shell Research Foundation, SenterNovem (EOSLT01013), and the European Commission (Fullspectrum project, contract no SES6-CT-2003-502620) for funding.

References and Notes

(1) O'Regan, B.; Grätzel, M. *Nature* **1991**, *353*, 737−739.
(2) Grätzel, M. *Nature* **2001**, *414*, 338−344.
(3) Grätzel, M. *J. Photochem. Photobiol. C: Photochem. Rev.* **2003**, *4*, 145−153.
(4) Späth, M.; Sommeling, P. M.; Roosmalen, J. A. M. v.; Smit, H. J. P.; Burg, N. P. G. v.d.; Mahieu, D. R.; Bakker, N. J.; Kroon, J. M. *Prog. Photovolt. Res. Appl.* **2003**, *11*, 207−220.
(5) Kroon J. M.; O'Regan, B. C.; Roosmalen, J. A. M. v.; Sinke, W. C. *Inorganic Photochemistry*; American Scientific Publishers: Stevenson Ranch, CA, 2003; Chapter 1, pp 1−47.
(6) Barbe, C. J.; Arendse, F.; Comte, P. *J. Am. Ceram. Soc.* **1997**, *80*, 3157−3171.
(7) Park, N. G.; Schlichthörl, G.; Lagemaat, J. v. d.; Cheong, H. M.; Mascarenhas, A.; Frank, A. J. *J. Phys. Chem. B* **1999**, *103*, 3308−3314.
(8) Nazeeruddin, M. K.; Kay, A.; Rodicio, I.; Humphry-Baker, R.; Müller, E.; Liska, P.; Vlachopoulos, N.; Grätzel, M. *J. Am. Chem. Soc.* **1993**, *115*, 6382−6390.
(9) Zeng, L. Y.; Dai, S. Y.; Wang, K. J.; Pan, X.; Shi, C. W.; Guo, L. *Chin. Phys. Lett.* **2004**, *21*, 1835−1837.
(10) Kavan, L.; O'Regan, B.; Kay, A.; Grätzel, M. *J. Electroanal. Chem.* **1993**, *346*, 291−307.
(11) Menzies, D.; Gervini, R.; Cheng, Y. B.; Simon, G. P.; Spiccia, L. *J. Aust. Ceram. Soc.* **2003**, *39* (2), 108−113.
(12) Ito, S.; Liska, P.; Comte, P.; Charvet, R. L.; Péchy, P.; Bach, U.; Schmidt-Mende, L.; Zakeeruddin, S. M.; Kay, A.; Nazeeruddin, M. K.; Grätzel, M. *Chem. Commun.* **2005**, 4351−4353.
(13) Kay, A. Solar cells based on dye-sensitized nanocrystalline TiO_2 electrodes. Thesis, Ecole Polytechnique Federale de Lausanne, 1994.
(14) Wang, P.; Zakeeruddin, S. M.; Comte, P.; Charvet, R.; Humphry-Baker, R.; tzel, M. *J. Phys. Chem. B* **2003**, *107*, 14336−14341.
(15) Kroon, J. M.; Bakker, N. J.; Smit, H. J. P.; Liska, P.; Thampi, K. R.; Wang, P.; Zakeeruddin, S. M.; Grätzel, M.; Hinsch, A.; Hore, S.; Würfel, U.; Sastrawan, R.; Durrant, J. R.; Palomares, E.; Pettersson, H.; Gruszecki, T.; Walter, J.; Skupien, K.; Tulloch, G. E. *Prog. Photovolt. Res. Appl.* **2006**, accepted.
(16) Hinsch, A.; Kroon, J. M.; Kern, R.; Uhlendorf, I.; Holzbock, J.; Meyer, A.; Ferber, J. *Prog. Photovolt. Res. Appl.* **2001**, *9*, 425−438.
(17) *Annual Books of ASTM Standards: Section 12: Nuclear, Solar and Geothermal Energy*; ASTM Intl: West Conshohocken, PA, 1995; Vol. 12.2, pp 573−577
(18) Sommeling, P. M.; Rieffe, H. C.; Roosmalen, J. A. M. v.; Schönecker, A.; Kroon, J. M.; Wienke, J. A.; Hinsch, A. *Sol. Energy Mater. Sol. Cells* **2000**, *62*, 399−410.
(19) O'Regan, B. C.; Scully, S.; Mayer, A. C.; Palomares, E.; Durrant, J. R. *J. Phys. Chem. B* **2005**, *109*, 4616−4623.
(20) O'Regan, B. C.; Lenzmann, F. *J. Phys. Chem. B* **2004**, *108*, 4342−4350.
(21) O'Regan, B. C.; Durrant, J. R. Web Release Date: 12 Apr, 2006.
(22) Zhang, Z.; Zakeeruddin, S. M.; O'Regan, B. C.; Humphry-Baker, R.; Gratzel, M. *J. Phys. Chem. B* **2005**, *109*, 21818−21824.
(23) O'Regan, B. C.; Sommeling, P. M.; Durrant, J. R. Manuscript in preparation.
(24) Palomares, E.; Clifford, J.; Haque, S. A.; Lutz, T.; Durrant, J. R. *J. Am. Chem. Soc.* **2003**, *125*, 475−482.
(25) Haque, S. A.; Palomares, E.; Cho, B. M.; Green, A. N. M.; Hirata, N.; Klug, D. R.; Durrant, J. R. *J. Am. Chem. Soc.* **2005**, *127*, 3456−3462.